Heliyon 5 (2019) e02499

Contents lists available at ScienceDirect

Heliyon

www.elsevier.com/locate/heliyon

Closed-form probability distribution of number of infections at a given time in a stochastic SIS epidemic model

Olusegun Michael Otunuga *

Department of Mathematics, Marshall University, One John Marshall Drive, Huntington, WV, USA

ARTICLE INFO

Keywords:
Applied mathematics
Epidemiology
Infection
Stochastic model
Differential equation
Laguerre
Fokker-Planck
Kummer
Epidemic model

ABSTRACT

We study the effects of external fluctuations in the transmission rate of certain diseases and how these affect the distribution of the number of infected individuals over time. To do this, we introduce random noise in the transmission rate in a deterministic SIS model and study how the number of infections changes over time. The objective of this work is to derive and analyze the closed form probability distribution of the number of infections at a given time in the resulting stochastic SIS epidemic model. Using the Fokker-Planck equation, we reduce the differential equation governing the number of infections to a generalized Laguerre differential equation. The properties of the distribution, together with the effect of noise intensity, are analyzed. The distribution is demonstrated using parameter values relevant to the transmission dynamics of influenza in the United States.

1. Introduction

Existing mathematical models [4, 6, 9, 10, 11, 13, 14, 15, 18, 21, 22, 23, 24] have been developed in order to understand the transmission and elimination of diseases. Several researchers [9, 10, 18, 21, 22, 23, 24] have shed light on the transmission dynamics of infectious diseases and its distribution. In this paper, we shed more light on how the number of infections of certain diseases (described using the well known SIS model) is distributed.

We first consider the deterministic SIS model for description of the population dynamics for certain diseases. The host population is partitioned into two compartments, the susceptible and infectious population, with sizes denoted by S and I, respectively. The total population $N(t) = S(t) + I(t)$. The model governing S and I is described by the system of differential equation:

$$\begin{cases} dS &= (\Lambda - \beta SI - \mu S + \gamma I)\,dt, \quad S(t_0) = S_0, \\ dI &= (\beta SI - (\mu+\gamma)I)\,dt, \quad I(t_0) = I_0, \end{cases} \tag{1.1}$$

where $S_0 \geq 0$, $I_0 \geq 0$, $\Lambda > 0$ is the recruitment rate, β is the transmission rate, μ is the natural death rate and γ is the temporary recovery rate. We note here that the model above is the well-known SIS model [6, 10]. The total population N satisfies the differential equation

$$dN = (\Lambda - \mu N)dt, \quad N(t_0) = N_0, \tag{1.2}$$

with solution $N(t) = \frac{\Lambda}{\mu} - \left(\frac{\Lambda}{\mu} - N_0\right)e^{-\mu(t-t_0)}$. It follows that $S_0 + I_0 = N_0$ and the total population $N = \frac{\Lambda}{\mu}$ if $N_0 = \frac{\Lambda}{\mu}$. Define $\kappa = \frac{\Lambda}{\mu}$. It is well known [6, 10] that the system of differential equation (1.1) has two equilibriums, namely, the disease-free, P_0, and endemic, P_1, equilibrium defined by

$$\begin{aligned} P_0 &= (\kappa, 0), \\ P_1 &= \left(\frac{\kappa}{R_0}, \left(1 - \frac{1}{R_0}\right)\kappa\right), \quad \text{provided} \quad R_0 > 1, \end{aligned} \tag{1.3}$$

respectively, where

$$R_0 = \frac{\beta\kappa}{\mu+\gamma}. \tag{1.4}$$

It can be shown (for better understanding of the SIS model, we refer the readers to the papers [4, 10, 21]) that the solution $(I(t), S(t))$ of (1.1) is given by

$$I(t) = \begin{cases} \frac{(\mu+\gamma)(R_0-1)I_0}{(\mu+\gamma)(R_0-1)e^{-(\mu+\gamma)(R_0-1)(t-t_0)} + \beta I_0\left(1 - e^{-(\mu+\gamma)(R_0-1)(t-t_0)}\right)}, & \text{if} \quad R_0 \neq 1, \\ \left(\beta(t-t_0) + \frac{1}{I_0}\right)^{-1}, & \text{if} \quad R_0 = 1, I_0 \neq 0, \end{cases} \tag{1.5}$$

* Corresponding author.
E-mail address: otunuga@marshall.edu.

https://doi.org/10.1016/j.heliyon.2019.e02499
Received 15 July 2019; Received in revised form 15 September 2019; Accepted 17 September 2019

$$S(t)=\begin{cases}\dfrac{\kappa(\mu+\gamma)(R_0-1)\left(e^{-(\mu+\gamma)(R_0-1)(t-t_0)}-I_0/\kappa\right)+\kappa\beta I_0\left(1-e^{-(\mu+\gamma)(R_0-1)(t-t_0)}\right)}{(\mu+\gamma)(R_0-1)e^{-(\mu+\gamma)(R_0-1)(t-t_0)}+\beta I_0\left(1-e^{-(\mu+\gamma)(R_0-1)(t-t_0)}\right)}, \\ \quad \text{if } R_0\neq 1, \\ \kappa-\left(\beta(t-t_0)+\dfrac{1}{I_0}\right)^{-1}, \quad \text{if } R_0=1, I_0\neq 0.\end{cases} \tag{1.6}$$

It follows directly that the equilibrium point P_0 is globally stable if $R_0\leq 1$ (that is, irrespective of the initial point, $I(t)\to 0$ and $S(t)\to\kappa$ as $t\to\infty$ if $R_0\leq 1$), and equilibrium point P_1 is globally stable if $R_0>1$ (that is, $I(t)\to\left(1-\frac{1}{R_0}\right)\kappa$ and $S(t)\to\kappa/R_0$ as $t\to\infty$ if $R_0>1$). The number R_0 is referred to as the reproduction number, which is the average number of secondary infection produced by an infectious individual when introduced into susceptible population. We can make the sizes S and I into percentages by setting $\Lambda=\mu$.

2. Background

2.1. Stochastic SIS model

We assume that external fluctuations may be caused by variability in the number of contacts between infected and susceptible individuals and such random variations can be modeled by a white noise [10]. We also assume that fluctuations will manifest mainly as fluctuations in the infectivity parameter β, and that the transmission rates fluctuate rapidly compared to the evolution of the disease. External noise appears multiplicatively and it is able to modify the mean dynamical behavior of the population. By allowing the infectivities to fluctuate around a mean value, we introduce external fluctuations in the model as follows:

$$\beta\equiv\beta+\sigma C(t), \tag{2.1}$$

where $C(t)$ is the noise term with zero mean. We assume that the transmission rate fluctuates rapidly so that we can model $C(t)$ by a standard Gaussian white noise. The constant σ is the noise intensity of the white noise due to fluctuations in infectivities of the disease. It represents measure of the amplitude of fluctuations in the transmission rate. By substituting (2.1) into (1.1), we get a Langevin equation. The approach of this equation gives rise to what we called a stochastic differential equation. It is important to be able to interprete and evaluate the noise structure of this equation. The Itô approach on stochastic differential equation depends on Markovian and Martingale properties. These properties do not obey the traditional chain rule. Whereas, the Stratonovich approach obeys the traditional chain rule and allows white noise to be treated as a regular derivative of a Brownian or Wiener process [6, 16, 20]. For this reason, by substituting (2.1) into (1.1), we extend the resulting equation to a Stratonovich stochastic model of the form

$$\begin{cases} dS &= (\Lambda-\beta SI-\mu S+\gamma I)\,dt-\sigma SI\circ dW(t), \quad S(t_0)=S_0 \\ dI &= (\beta SI-(\mu+\gamma)I)\,dt+\sigma SI\circ dW(t), \quad I(t_0)=I_0 \end{cases} \tag{2.2}$$

where $S_0\geq 0$, $I_0\geq 0$, $W(t)$ is a standard Wiener process on a filtered probability space $(\Omega,\mathcal{F}_t,(\mathcal{F}_t)_{t\geq 0},\mathbb{P})$, the filtration function $(\mathcal{F}_t)_{t\geq 0}$ is right-continuous and each $\mathcal{F}_t$ with $t\geq 0$ contains all $\mathbb{P}$-null sets in $\mathcal{F}_t$; $\circ$ denotes the Stratonovich integral [2]. The initial process $x(t_0)=(S_0,I_0)$ is $\mathcal{F}_{t_0}$ measurable and independent of $W(t)-W(t_0)$.

The stochastic differential equation has a unique positive solution $I(t)\in(0,\kappa)$ [4, 10, 13, 21] in the feasible region

$$\mathcal{T}:=\left\{(S,I)\in\mathbb{R}_+\mid 0\leq S+I\leq\kappa\right\} \tag{2.3}$$

for all $t\geq 0$ with probability one. By setting $S=\kappa-I$, the stochastic differential equation governing I in (2.2) reduces to

$$dI=(\beta(\kappa-I)I-(\mu+\gamma)I)\,dt+\sigma(\kappa-I)I\circ dW(t), \quad I(t_0)=I_0. \tag{2.4}$$

We use the Stratonovich-Itô conversion theorem given in Bernardi et al. [3] and Kloeden et al. [8] to convert the Stratonovich dynamic model (2.4) into its Itô's equivalent

$$dI=\left(\boldsymbol{\mu}(I)+\frac{1}{2}\boldsymbol{\sigma}'_{1,1}(I)\boldsymbol{\sigma}_{1,1}(I)\right)dt+\boldsymbol{\sigma}_{1,1}(I)\,dW(t), \quad I(t_0)=I_0, \tag{2.5}$$

where

$$\boldsymbol{\mu}(I)=\beta(\kappa-I)I-(\mu+\gamma)I,$$

$$\boldsymbol{\sigma}_{1,1}(I)=\sigma(\kappa-I)I,$$

are the drift and diffusion coefficients of (2.4), respectively.

2.2. Classification of the boundaries of diffusion process I in $\mathcal{T}$

We classify the boundaries $I=I_0=0$ and $I=\kappa$ using the definitions provided in Horsthemke et al. [6] and Méndez et al. [10].

Definition 1. ([6, 10]) Let $\bar{b}$ be a boundary point and b^* be a point near $\bar{b}$. The classification of boundary $\bar{b}$ is based on the integrability of the function $\phi(x)$ defined by

$$\phi(x)=\exp\left(-\int_{b^*}^{x}\frac{2\left(\boldsymbol{\mu}(z)+\frac{1}{2}\boldsymbol{\sigma}'_{1,1}(z)\boldsymbol{\sigma}_{1,1}(z)\right)}{\boldsymbol{\sigma}^2_{1,1}(z)}\,dz\right). \tag{2.6}$$

The boundary $\bar{b}$ is natural if it is attained with probability zero even if time goes to infinity. Analytically, the boundary $\bar{b}$ is natural if and only if the integral $L_1(\bar{b})=\int_{\bar{b}}^{b^*}\phi(x)\,dx=c\int_{\bar{b}}^{b^*}x^{-(\bar{A}+2)}(\kappa-x)^{\bar{A}}e^{\frac{\bar{C}}{\kappa-x}}\,dx$ diverges [6, 10], where we define

$$\begin{aligned}\bar{A} &= \tfrac{2}{\sigma^2\kappa^2}\left(\beta\kappa-(\mu+\gamma)-\sigma^2\kappa^2/2\right), \\ \bar{B} &= \bar{A}+2, \\ \bar{C} &= \tfrac{2}{\sigma^2\kappa^2}(\mu+\gamma).\end{aligned} \tag{2.7}$$

Since

$$L_1(u)=\int_u^{u+\epsilon}\phi(x)\,dx=\frac{(\kappa\bar{C})^{\bar{A}+1}}{\kappa^{\bar{B}}}e^{\bar{C}}\int_{\bar{C}\frac{u}{\kappa-u}}^{\bar{C}\frac{u+\epsilon}{\kappa-[u+\epsilon]}}\omega^{-\bar{B}}e^{\omega}\,d\omega$$

$$=\frac{(\kappa\bar{C})^{\bar{A}+1}}{(-\kappa)^{\bar{B}}}e^{-\bar{C}}\left[\Gamma\left(1-\bar{B},-\bar{C}\frac{u+\epsilon}{\kappa-[u+\epsilon]}\right)-\Gamma\left(1-\bar{B},-\bar{C}\frac{u}{\kappa-u}\right)\right]$$

exists if $1-\bar{B}>0$, where $\Gamma(s,\nu)=\int_\nu^\infty t^{s-1}e^{-t}\,dt$ is the upper Incomplete Gamma function, it follows directly from Definition 1 that the boundary $I=0$ is natural if $1-\bar{B}<0$, that is, if $R_0>1$. Likewise, the upper boundary κ is natural for all values of the parameters [10]. Hence, we conclude that the boundaries $I_0=0$ and $I=\kappa$ are unattainable at all times if $R_0>1$, regardless of the noise intensity.

Definition 2. ([6, 10]) A boundary $\bar{b}$ is called attracting if when the process $I(t)$ starts at $t=0$ at $I_0\in(\bar{b},b^*)$, it either leaves this interval in a finite time τ_{I_0} (in this case via the right point), or it never leaves this interval and then $I(t)\to\bar{b}$ as $t\to\infty$. Analytically, the boundary $\bar{b}$ is attracting if $L_1(\bar{b})<\infty$ and $L_2(\bar{b})=\int_{\bar{b}}^{b^*}\frac{2}{\sigma^2_{1,1}(y)}\int_{\bar{b}}^{y}\phi(x)dx\,\phi^{-1}(y)\,dy=\infty$ [6, 10].

It follows that the boundary $I=0$ is attracting if $R_0<1$ [10]. Since $I_0=0$ is an equilibrium point of (2.4), this means that the stationary probability will be concentrated entirely on $I_0=0$, that is, $P_s(I)=\delta(I)$ if $R_0<1$, where P_s and δ denote the stationary probability distribution and dirac delta function, respectively.

2.3. Closed form solution of (2.5)

Using the change of state variable

$$x=\bar{C}\frac{I}{\kappa-I} \tag{2.8}$$

in (2.5), we obtain the Itô stochastic differential equation

$$dx = \frac{\sigma^2\kappa^2}{2} x\left(\bar{\mathcal{A}} + 2 - x\right)\, dt + \sigma\kappa x\, dW(t). \tag{2.9}$$

A second change of variable

$$y = 1/x \tag{2.10}$$

reduces (2.9) to

$$dy = \frac{\sigma^2\kappa^2}{2}\left(1 - \bar{\mathcal{A}} y\right)\, dt - \sigma\kappa y\, dW(t). \tag{2.11}$$

Equation (2.11) is the well known geometric stochastic differential equation with solution

$$y(t) = y_0\Phi(t,t_0) + \frac{\sigma^2\kappa^2}{2}\Phi(t,t_0)\int_{t_0}^{t}\Phi^{-1}(s,t_0)\, ds, \tag{2.12}$$

where

$$\begin{aligned}\Phi(t,t_0) &= e^{-\frac{\sigma^2\kappa^2}{2}(\bar{\mathcal{A}}+1)(t-t_0)-\sigma\kappa\left(W(t)-W(t_0)\right)}\\ &= e^{-(\mu+\gamma)(R_0-1)(t-t_0)-\sigma\kappa\left(W(t)-W(t_0)\right)},\end{aligned} \tag{2.13}$$

with mean value

$$\mathbb{E}\left(\Phi(t,t_0)\right) = e^{-\frac{\sigma^2\kappa^2}{2}(\bar{\mathcal{A}})(t-t_0)}.$$

We note from (2.7) that $\bar{\mathcal{A}} = \bar{C}\left(\bar{R}_0 - 1\right)$, where

$$\begin{aligned}\bar{R}_0 &= \frac{\beta\kappa - \sigma^2\kappa^2/2}{\mu+\gamma}\\ &= R_0 - \frac{1}{\bar{C}}.\end{aligned} \tag{2.14}$$

It follows from (2.8) and (2.10) that the solution $I(t) = \frac{\kappa x(t)}{x(t)+\bar{C}} = \frac{\kappa}{1+\bar{C}y(t)}$ is given by

$$I(t) = \frac{\kappa}{1 + \bar{C}\left(y_0\Phi(t,t_0) + \frac{\sigma^2\kappa^2}{2}\Phi(t,t_0)\int_{t_0}^{t}\Phi^{-1}(s,t_0)\, ds\right)}. \tag{2.15}$$

It was shown in Gray et al. [4] that disease dies out with probability one (that is, $I(t) \to 0$ exponentially, almost surely) if $\bar{R}_0 < 1$ and $\sigma^2 \le \beta/\kappa$. Likewise, in their work, Tornatore et al. [15] showed that if $\min\{\mu+\gamma-\sigma^2\kappa^2/2, 2\mu\} < \beta\kappa < \mu+\gamma+\sigma^2\kappa^2/2\}$, the disease-free equilibrium point $P_0 = (\kappa, 0)$ of (2.2) is globally stable in the feasible region $\mathcal{T}$ and unstable if $\bar{R}_0 > 1$. They state from biological point of view that the introduction of a noise in the deterministic SIS model (1.1) modifies the deterministic stability threshold of the disease-free equilibrium. As $\sigma \to 0^+$, $\Phi(t,t_0) \to e^{-(\mu+\gamma)(R_0-1)(t-t_0)}$ and $\bar{R}_0 \to R_0$. In this case, the system (2.5) reduces to (1.1). More results on the effect of the noise intensity on disease dynamics are discussed in Remark 3.

3. Model

3.1. Probability distribution of infectious diseases: SIS model

Using the change of variable described in (2.8), we define $P(x,t|x_0)$ as the probability of x at time t given the initial point x_0. In this Section, we derive the closed form distribution $P(x,t|x_0)$ and later extends the result to derive the closed form probability $P(I,t|I_0)$ that the number of infected individuals is I at time t, given initial point I_0.

Let $h(x)$ and $g(x)$ be the drift and diffusion coefficients of (2.9) defined by

$$\begin{aligned}h(x) &= \frac{\sigma^2\kappa^2}{2} x\left(\bar{\mathcal{A}} + 2 - x\right),\\ g(x) &= \sigma\kappa x.\end{aligned} \tag{3.1}$$

The probability density $P(x,t|x_0)$ satisfies the Fokker-Planck equation

$$\frac{\partial P}{\partial t} = -\frac{\partial}{\partial x}\{h(x)P\} + \frac{1}{2}\frac{\partial}{\partial x}\left\{g^2(x)P\right\}, \quad 0 < t < \infty. \tag{3.2}$$

We seek a solution of (3.2) of the form

$$P(x,t|x_0) = T(t)\Psi(x|x_0). \tag{3.3}$$

To find a solution, we consider a case where a stationary probability density exists and is unique. This is satisfied when the boundaries are either natural or regular boundaries, with instantaneous reflection [6]. By substituting (3.3) into (3.2), we have

$$\frac{1}{T}\frac{dT}{dt} = \frac{1}{\Psi}\left(-\frac{d}{dx}\{h(x)\Psi(x)\} + \frac{1}{2}\frac{d^2}{dx^2}\left\{g^2(x)\Psi(x)\right\}\right).$$

The above equation is possible if each side is a constant, say, $-r$, so that $T(t) = e^{-rt}$ and

$$-\frac{d}{dx}\{h(x)\Psi(x)\} + \frac{1}{2}\frac{d^2}{dx^2}\left\{g^2(x)\Psi(x)\right\} = -r\Psi(x), \tag{3.4}$$

with boundary condition

$$-\frac{\sigma^2\kappa^2}{2}\frac{d}{dx}\left(x^2\Psi(x)\right) + h(x)\Psi(x)|_{x=0,\infty} = 0, \tag{3.5}$$

that is, we assume there is no probability flux at the boundary. The values of r, for which a function $\Psi(x) \equiv \Psi_r(x)$ exists and do not vanish identically in the interval $(0,\infty)$ and which fulfils (3.4)-(3.5) are called the eigenvalues [6]. The corresponding solutions $\Psi_r(x)$ are called eigenfunctions.

Let $P_s(x)$ be the unique stationary probability density satisfying

$$-h(x)P_s(x) + \frac{1}{2}\frac{d}{dx}\left\{g^2(x)P_s(x)\right\} = 0. \tag{3.6}$$

It can be shown that the solution $P_s(x)$ satisfying (3.6) is obtained as

$$P_s(x) = \frac{1}{\Gamma(\bar{\mathcal{A}}+1)} x^{\bar{\mathcal{A}}} e^{-x}, \quad 0 < x < \infty, \tag{3.7}$$

provided $\bar{\mathcal{A}} + 1 > 0$, or equivalently, $R_0 > 1$. This is a Gamma distribution with a unit rate parameter. We convert the eigenvalue problem for the Fokker-Planck equation into a Sturm-Liouville problem by setting $\Psi(x)$ to

$$\Psi(x) = P_s(x)f(x), \quad 0 < x < \infty, \tag{3.8}$$

for some function $f(x)$, and substituting into (3.4) to obtain

$$\frac{\sigma^2\kappa^2}{2}\frac{d}{dx}\left(x^2 P_s(x)\frac{d}{dx}f(x)\right) + rP_s(x)f(x) = 0, \tag{3.9}$$

with boundary condition

$$\left(x^2 P_s(x)\frac{d}{dx}f(x)\right)|_{x=0,\infty} = 0. \tag{3.10}$$

Note that (3.9) is the Kolmogorov backward equation with eigenvalue r, which is the same as the eigenvalue of the Fokker-Planck equation (3.4). The eigenfunctions of the Fokker-Planck equation and Kolmogorov backward equation are related by the relation (3.8). According to Horsthemke et al. [6], all eigenvalues are real and nonnegative. Furthermore, since both boundaries (0 and κ) for I are finite, we have a discrete range of eigenvalues, including $r = 0$ since we assume that the stationary probability density is unique. Define

$$\begin{aligned}q &= (\beta\kappa - (\mu+\gamma))^2 - 2\sigma^2\kappa^2 r,\\ \lambda &= \frac{1}{\sigma^2\kappa^2}\left(\beta\kappa - (\mu+\gamma) - \sqrt{q}\right),\\ \alpha &= \frac{2\sqrt{q}}{\sigma^2\kappa^2}.\end{aligned} \tag{3.11}$$

It follows immediately from (3.11) that

$$\alpha = \bar{\mathcal{A}} - 2\lambda + 1. \tag{3.12}$$

We shall later show that $q > 0$ under suitable condition. By substituting

$$f(x) = x^{-\lambda}\, y(x), \quad 0 < x < \infty, \tag{3.13}$$

into (3.9) for some function $y(x)$, we obtain the differential equation

$$xy'' + (1+\alpha - x)y' + \lambda y = 0, \tag{3.14}$$

where α and λ are given in (3.11). Equation (3.14) is the well known Kummer's equation (see Abramowitz and Stegun [1], Section 13.1.1; and Olver et al. [12], Section 13.2.1). The solution becomes the generalized/associated Laguerre polynomial of degree λ if λ is a nonnegative integer. The general solution of (3.14) is given by

$$y(x) = C_1 U(-\lambda, 1+\alpha, x) + C_2 M(-\lambda, 1+\alpha, x), \quad 0 < x < \infty, \tag{3.15}$$

where $U(a,b,z)$ is the confluent hypergeometric function [1, 12] and $M(a,b,z)$ is the Kummer's function (see [1] Section 13.1.2). Using relation

$$M(-\lambda, 1+\alpha, z) = \frac{\lambda!}{(1+\alpha)_\lambda} L(\lambda, \alpha, z),$$

where $(a)_k$ is the Pochhammer's symbol (or shifted factorial) [12] and $L(a,b,z)$ is the generalized Laguerre function [7], we can rewrite (3.15) in the form

$$y(x) = C_1 U(-\lambda, 1+\alpha, x) + C_2 L(\lambda, \alpha, x), \quad 0 < x < \infty. \tag{3.16}$$

Hence, the solutions $f(x)$ and $\Psi(x)$ in (3.13) and (3.8) reduce to

$$f(x) = C_1 x^{-\lambda} U(-\lambda, 1+\alpha, x) + C_2 x^{-\lambda} L(\lambda, \alpha, x), \quad 0 < x < \infty, \tag{3.17}$$

and

$$\Psi(x) = \frac{1}{\Gamma(\bar{\mathcal{A}}+1)} x^{\bar{\mathcal{A}}-\lambda} e^{-x} \left(C_1 U(-\lambda, 1+\alpha, x) + C_2 L(\lambda, \alpha, x) \right), \quad 0 < x < \infty. \tag{3.18}$$

If $\lambda = n$ is a nonnegative integer, it follows immediately from (3.11) that the eigenvalue $r \equiv r_n$ is obtained as

$$\begin{aligned} r_n &= n(\beta\kappa - (\mu+\gamma)) - n^2 \frac{\sigma^2\kappa^2}{2} = \frac{\sigma^2\kappa^2}{2}(n^2 + \alpha_n n), \\ &= \frac{\sigma^2\kappa^2}{2}\left(\bar{\mathcal{A}} + 1 - n\right) n, \quad \text{for } 0 \le n \le M, \end{aligned} \tag{3.19}$$

where $M = \left\lfloor \frac{\beta\kappa - (\mu+\gamma)}{\sigma^2\kappa^2} \right\rfloor = \left\lfloor \frac{\bar{\mathcal{A}}+1}{2} \right\rfloor$ and $\lfloor . \rfloor$ is the floor function. Thus,

$$\begin{aligned} q \equiv q_n &= \left(\beta\kappa - (\mu+\gamma) - n\sigma^2\kappa^2\right)^2, \\ \alpha \equiv \alpha_n &= \frac{2}{\sigma^2\kappa^2}\sqrt{q_n} = \frac{2}{\sigma^2\kappa^2}\left(\beta\kappa - (\mu+\gamma) - n\sigma^2\kappa^2\right) > 0, \end{aligned} \tag{3.20}$$

provided $\bar{\mathcal{A}} + 1 - 2n > 0$. Clearly, $r_n \ge 0$ since $\alpha_n = \bar{\mathcal{A}} + 1 - 2n$. For the rest of this work, we assume that

$$\bar{\mathcal{A}} - 2\lambda + 1 > 0. \tag{3.21}$$

Using relation (13.6.19) in [12], we can write $U(-\lambda, 1+\alpha, x)$ in terms of $L(\lambda, \alpha, x)$. The eigenfunction $f(x) \equiv f_n(x)$ of the eigenvalue problem (3.9) now reduces to

$$f_n(x) = Z_n x^{-n} L\left(n, \alpha_n, x\right), \tag{3.22}$$

where Z_n is a normalization constant and $\alpha \equiv \alpha_n$ is given in (3.12). Using (3.12) and the explicit representation identities for Laguerre polynomials (see [12] Section 18.5.12, [5] Vol 1 Section 2.1.1(2) and [5] Vol 2 Section 10.12.33)

$$\begin{cases} L(n, \alpha_n, x) &= \sum_{i=0}^{n} \frac{(\alpha_n + i + 1)_{n-i}}{i!(n-i)!}(-x)^i, \\ \int_0^\infty x^{\nu-1} e^{-x} L(n, \alpha_n, x)\, dx &= \left(\frac{\Gamma(\nu)\Gamma(\alpha_n + n + 1)}{n!\Gamma(\alpha_n + 1)}\right) {}_2F_1(-n, \nu; \alpha_n + 1; 1), \text{ if } \nu > 0, \end{cases}$$

where ${}_2F_1(a_1, a_2; b; z)$ is the generalized hypergeometric function (see [12] Section 16.1.1), it follows that

$$\int_0^\infty x^{\bar{\mathcal{A}}-2n} e^{-x} L(n, \alpha_n, x)^2\, dx = \frac{\Gamma(\alpha_n + n + 1)^2}{\Gamma(\alpha_n + 1) n!} \sum_{i=0}^{n} (-1)^i \left(\frac{{}_2F_1(-n, \alpha_n + i; \alpha_n + 1; 1)}{i!(n-i)!(\alpha_n + i)} \right) = D_n^{-1},$$

provided condition (3.21) is satisfied. Since the eigenfunctions of the Fokker-Planck differential equation are orthogonal with respect to $1/P_s(x)$ [6, 19], we use the above result to normalize the eigenfunctions $f_n(x)$ by calculating the value of Z_n using the orthogonal conditions

$$\begin{aligned} \int_0^\infty P_s(x) f_n(x) f_m(x)\, dx &= 0, \text{ for } n \ne m, \\ \int_0^\infty P_s(x) f_n(x)^2\, dx &= \frac{1}{\Gamma(\bar{\mathcal{A}}+1)} D_n^{-1}. \end{aligned} \tag{3.23}$$

Thus, $Z_n = \sqrt{\Gamma(\bar{\mathcal{A}}+1) D_n}$. We also note here that the eigenvalues derived in (3.19) can be obtained from the integral [19] as

$$r_n = \int_0^\infty \frac{1}{2} g^2(x) P_s(x) \left[\frac{df_n(x)}{dx}\right]^2 dx,$$

using (3.9) and (3.10), where $g(x)$ is the diffusion coefficient in (3.1). The solution $P(x,t|x_0)$ of (3.2) is obtained as

$$P(x,t|x_0) = P_s(x) \sum_{n=0}^{M} e^{-r_n t} f_n(x_0) f_n(x), \quad 0 < x < \infty. \tag{3.24}$$

Transforming back to the original variable I using (2.8), we obtain the probability

$$\begin{aligned} &P(I,t|I_0) \\ &= P(x(I),t|x(I_0)) \left|\frac{dx}{dI}\right| \\ &= \kappa \bar{C}^{\bar{\mathcal{A}}+1} \frac{I^{\bar{\mathcal{A}}}}{(\kappa - I)^{\bar{\mathcal{B}}}} e^{-\frac{\bar{C}I}{\kappa - I}} \\ &\quad \times \sum_{n=0}^{M} D_n e^{-r_n t} \left(\frac{\bar{C}I_0}{\kappa - I_0}\frac{\bar{C}I}{\kappa - I}\right)^{-n} L\left(n, \alpha_n, \frac{\bar{C}I_0}{\kappa - I_0}\right) L\left(n, \alpha_n, \frac{\bar{C}I}{\kappa - I}\right), \\ &\quad 0 < I < \kappa, \end{aligned} \tag{3.25}$$

and

$$\begin{aligned} &P(S,t|S_0) \\ &= \kappa \bar{C}^{\bar{\mathcal{A}}+1} \frac{(\kappa - S)^{\bar{\mathcal{A}}}}{S^{\bar{\mathcal{B}}}} e^{-\frac{\bar{C}(\kappa - S)}{S}} \\ &\quad \times \sum_{n=0}^{M} D_n e^{-r_n t} \left(\frac{\bar{C}(\kappa - S_0)}{S_0}\frac{\bar{C}(\kappa - S)}{S}\right)^{-n} L\left(n, \alpha_n, \frac{\bar{C}(\kappa - S_0)}{S_0}\right) \\ &\quad \times L\left(n, \alpha_n, \frac{\bar{C}(\kappa - S)}{S}\right), \quad 0 < S < \kappa, \end{aligned} \tag{3.26}$$

since $S + I = \kappa$.

3.2. Properties of the distribution $P(x,t|x_0)$

We discuss some properties, namely, the mean, median, mode, variance, skewness, moment generating function, and characteristic function for the density function $P(x,t|x_0)$.

In general, the j-th moment, $\mu_x^{(j)}(t)$, of the density $P(x,t|x_0)$ is given by

$$\begin{aligned} \mu_x^{(j)}(t) &= \int_0^\infty x^j P(x,t|x_0)\, dx \\ &= \sum_{n=0}^{M} \frac{\Gamma(\alpha_n + n + j)\Gamma(\alpha_n + n + 1)}{\Gamma(\bar{\mathcal{A}}+1)\Gamma(\alpha_n + 1) n!} Z_n f_n(x_0) e^{-r_n t} {}_2F_1(-n, \alpha_n + n + j; \alpha_n + 1; 1). \end{aligned} \tag{3.27}$$

The mean $\mu_x^{(1)}(t)$, variance $\sigma_x^2(t) = \mu_x^{(2)}(t) - \left(\mu_x^{(1)}(t)\right)^2$, and skewness $\mathrm{sk}_x(t) = \mathbb{E}\left[\left(x - \mu_x^{(1)}\right)^3\right] / \sigma_x^3(t)$, of the distribution $P(x,t|x_0)$ can easily be calculated from (3.27) as

$$\begin{aligned}\mu_x^{(1)}(t) &= \sum_{n=0}^{M}\frac{\Gamma(\alpha_n+n+1)^2}{\Gamma(\bar{\mathcal{A}}+1)\Gamma(\alpha_n+1)n!}Z_n f_n(x_0)e^{-r_n t}\,{}_2F_1(-n,\alpha_n+n+1;\alpha_n+1;1),\\ \sigma_x^2(t) &= \sum_{n=0}^{M}\frac{\Gamma(\alpha_n+n+2)\Gamma(\alpha_n+n+1)}{\Gamma(\bar{\mathcal{A}}+1)\Gamma(\alpha_n+1)n!}Z_n f_n(x_0)e^{-r_n t}\,{}_2F_1(-n,\alpha_n+n+2;\alpha_n+1;1)\\ &\quad-\left(\mu_x^{(1)}(t)\right)^2,\\ \mathrm{sk}_x(t) &= \frac{\mu_x^{(3)}(t)-3\mu_x^{(2)}(t)\mu_x^{(1)}(t)+2\left(\mu_x^{(1)}(t)\right)^3}{\left(\sigma_x^2(t)\right)^{3/2}}.\end{aligned}\tag{3.28}$$

The mode, $\mathrm{mode}_x(t)=\arg\max_z P(z,t|x_0)$, of the distribution $P(x,t|x_0)$ is given by

$$\mathrm{mode}_x(t)=\left\{z>0\ :\ \sum_{n=0}^{M}e^{-r_n t}f_n(x_0)Z_n z^{-n}\big((\bar{\mathcal{A}}-n-z)L(n,\alpha_n,z)-zL(n-1,\alpha_n+1,z)\big)=0\right\},\tag{3.29}$$

where $L(n-1,\alpha_n+1,z)=L(n,\alpha_n+1,z)-L(n,\alpha_n,z)$. The median, $\mathrm{median}_x(t)$ at time t is the number $\bar{m}$ such that $\int_0^{\bar{m}}P(x,t|x_0)\,dx=1/2$. It satisfies

$$\mathrm{median}_x(t)=\left\{\bar{m}>0\ :\ \sum_{n=0}^{M}\sum_{j=0}^{n}e^{-r_n t}f_n(x_0)\times Z_n\frac{\Gamma(\alpha_n+n+1)}{\Gamma(\alpha_n+1+j)j!(n-j)!\Gamma(\bar{\mathcal{A}}+1)}(-1)^j\gamma\big(\bar{\mathcal{A}}-n+1+j,\bar{m}\big)=\frac{1}{2}\right\},\tag{3.30}$$

where $\gamma(s,x)=\int_0^x t^{s-1}e^{-t}\,dt$ is the lower incomplete Gamma function.

For fixed time t, the moment generating function $\mathrm{MGF}_t(\tau)=\mathbb{E}\left(e^{\tau x}P(x,t|x_0)\right)$ is given by

$$\mathrm{MGF}_t(\tau)=\sum_{n=0}^{M}\frac{\Gamma(\alpha_n+n)\Gamma(\alpha_n+n+1)}{\Gamma(\bar{\mathcal{A}}+1)\Gamma(\alpha_n+1)n!(1-\tau)^{\alpha_n+n}}\times Z_n f_n(x_0)e^{-r_n t}\,{}_2F_1\left(-n,\alpha_n+n;\alpha_n+1;\frac{1}{1-\tau}\right),\ \text{for } \tau<1.\tag{3.31}$$

The characteristic function $\mathrm{CF}_t(\tau)$ can be derived in a similar way.

3.2.1. Limiting distribution and statistics of the distribution $P(x,t|x_0)$

It is easy to show that as $t\to\infty$,

$$\begin{aligned}P(x,t|x_0) &\to P_s(x),\\ \mu_x^{(1)}(t) &\to \bar{\mathcal{A}}+1,\\ \sigma_x^2(t) &\to \bar{\mathcal{A}}+1,\\ \mathrm{sk}_x(t) &\to 2(\bar{\mathcal{A}}+1)^{-1/2},\\ \mathrm{mode}_x(t) &\to \bar{\mathcal{A}},\end{aligned}\tag{3.32}$$

and $\mathrm{median}_x(t)\to\hat{m}$, where $\hat{m}$ is the solution of the equation $\gamma\left(\bar{\mathcal{A}}+1,\hat{m}\right)=\Gamma\left(\bar{\mathcal{A}}+1\right)/2$, and $\gamma(s,x)$ is the incomplete Gamma function. It follows from (3.32) that the graph of the distribution $P(x,t|x_0)$ skewed to the right on the long run with skewness $2(\bar{\mathcal{A}}+1)^{-1/2}$, the mean and variance of the distribution converges to the same value $\bar{\mathcal{A}}+1$ on the long run. The number $\bar{\mathcal{A}}$ appears most (mode) on the long run.

3.3. Properties of the distribution $P(I,t|I_0)$

The j-th moment, $\mu_I^{(j)}(t)$, of the distribution $P(I,t|I_0)$ is given by

$$\begin{aligned}\mu_I^{(j)}(t) &= \int_0^\infty I^j P(I,t|I_0)\,dI\\ &= \sum_{n=0}^{M}\kappa^j D_n e^{-r_n t}\left(\frac{CI_0}{\kappa-I_0}\right)^{-n}L\left(n,\alpha_n,\frac{CI_0}{\kappa-I_0}\right)\\ &\quad\times\int_0^\infty\frac{u^{\bar{\mathcal{A}}+j-n}}{(u+\bar{C})^j}e^{-u}L(n,\alpha_n,u)\,du.\end{aligned}\tag{3.33}$$

The mean $\mu_I^{(1)}(t)$, variance $\sigma_I^2(t)=\mu_I^{(2)}(t)-\left(\mu_I^{(1)}(t)\right)^2$, and skewness $\mathrm{sk}_I(t)=\mathbb{E}\left[\left(I-\mu_I^{(1)}\right)^3\right]/\sigma_I^3(t)$, of the distribution $P(I,t|I_0)$ can easily be calculated from (3.33) as

$$\begin{aligned}\mu_I^{(1)}(t) &= \sum_{n=0}^{M}\kappa D_n e^{-r_n t}\left(\frac{CI_0}{\kappa-I_0}\right)^{-n}L\left(n,\alpha_n,\frac{CI_0}{\kappa-I_0}\right)\\ &\quad\times\int_0^\infty\frac{u^{\bar{\mathcal{A}}+1-n}}{u+\bar{C}}e^{-u}L(n,\alpha_n,u)\,du,\\ \sigma_I^2(t) &= \sum_{n=0}^{M}\kappa^2 D_n e^{-r_n t}\left(\frac{CI_0}{\kappa-I_0}\right)^{-n}L\left(n,\alpha_n,\frac{CI_0}{\kappa-I_0}\right)\\ &\quad\times\int_0^\infty\frac{u^{\bar{\mathcal{A}}+2-n}}{(u+\bar{C})^2}e^{-u}L(n,\alpha_n,u)\,du-\left(\mu_I^{(1)}(t)\right)^2,\\ \mathrm{sk}_I(t) &= \frac{\mu_I^{(3)}(t)-3\mu_I^{(2)}(t)\mu_I^{(1)}(t)+2\left(\mu_I^{(1)}(t)\right)^3}{\left(\sigma_I^2(t)\right)^{3/2}}.\end{aligned}\tag{3.34}$$

The mode, $\mathrm{mode}_I(t)$, is the argument, $\arg\max_I P(I,t|I_0)$, of the distribution $P(I,t|I_0)$. The median, $\mathrm{median}_I(t)$, at time t is the number $\hat{m}$ such that $\int_0^{\hat{m}}P(I,t|I_0)\,dI=1/2$. The number $\hat{m}$ satisfies the equation

$$\sum_{n=0}^{M}D_n e^{-r_n t}\left(\frac{\bar{C}I_0}{\kappa-I_0}\right)^{-n}L\left(n,\alpha_n,\frac{\bar{C}I_0}{\kappa-I_0}\right)\int_0^{\frac{\bar{C}\hat{m}}{\kappa-\hat{m}}}u^{\bar{\mathcal{A}}-n}e^{-u}L(n,\alpha_n,u)\,du=1/2.$$

For fixed time t, the moment generating function $\mathrm{MGF}_t(\tau)=\mathbb{E}\left(e^{\tau I}P(I,t|I_0)\right)$ is given by

$$\mathrm{MGF}_t(\tau)=\sum_{n=0}^{M}D_n e^{-r_n t}\left(\frac{\bar{C}I_0}{\kappa-I_0}\right)^{-n}L\left(n,\alpha_n,\frac{\bar{C}I_0}{\kappa-I_0}\right)\times\int_0^\infty u^{\bar{\mathcal{A}}-n}e^{-\frac{u(u-\bar{C}-\tau\kappa)}{u+\bar{C}}}L(n,\alpha_n,u)\,du.\tag{3.35}$$

Remark 1. Using change of variable, the stationary distribution

$$\begin{aligned}P_s(I) &= P_s(x(I))\left|\frac{dx}{dI}\right|,\\ &= \frac{\kappa\bar{C}^{\bar{\mathcal{A}}+1}}{\Gamma(\bar{\mathcal{A}}+1)}\frac{I^{\bar{\mathcal{A}}}}{(\kappa-I)^{\bar{\mathcal{B}}}}e^{-\frac{\bar{C}I}{\kappa-I}}.\end{aligned}\tag{3.36}$$

In this case, the expected number of infection

$$\begin{aligned}\mathbb{E}[I] &= \int_0^\kappa I P_s(I)\,dI=\frac{\kappa\bar{C}^{\bar{\mathcal{A}}+1}}{\Gamma(\bar{\mathcal{A}}+1)}\int_0^\kappa\left(\frac{I^{1+\bar{\mathcal{A}}}}{(\kappa-I)^{\bar{\mathcal{B}}}}\right)e^{-\frac{\bar{C}I}{\kappa-I}}\,dI\\ &= \frac{\kappa/\bar{C}}{\Gamma(\bar{\mathcal{A}}+1)}\int_0^\infty t^{1+\bar{\mathcal{A}}}\left(1+\frac{t}{\bar{C}}\right)^{-1}e^{-t}\,dt\\ &= P_0\,\kappa^{1+\bar{\mathcal{A}}/2}(\kappa\bar{C})^{1+\bar{\mathcal{A}}/2-\bar{\mathcal{B}}}\Gamma(2+\bar{\mathcal{A}})e^{-z/2}W_{p,m}(z),\end{aligned}$$

where $P_0=\frac{\kappa(\bar{C})^{\bar{\mathcal{A}}+1}e^{\bar{C}}}{\Gamma(1+\bar{\mathcal{A}})}$, $z=\bar{C}$, $p=-1-\bar{\mathcal{A}}/2$, $m=\left(1+\bar{\mathcal{A}}\right)/2$ and $W_{p,m}(z)=\frac{e^{-z/2}z^p}{\Gamma(1/2-p+m)}\int_0^\infty t^{-p-1/2+m}\left(1+\frac{t}{z}\right)^{p-1/2+m}e^{-t}\,dt$ is the Whittaker function [17]. Since $\kappa=S+I$, it follows that $\mathbb{E}[S]=\kappa-\mathbb{E}[I]$.

Remark 2. If $\bar{R}_0=1$, where $\bar{R}_0$ is defined in (2.14), then $M=0$, $\bar{\mathcal{A}}=0$, $\bar{\mathcal{B}}=2$, $P(x,t|x_0)\equiv P_s(x)\equiv e^{-x}$, $0<x<\infty$, $P(I,t|I_0)\equiv P_s(I)\equiv\frac{\kappa\bar{C}}{(\kappa-I)^2}e^{-\frac{\bar{C}I}{\kappa-I}}$, $0<I<\kappa$ and $P_s(S)\equiv\frac{\kappa\bar{C}}{S^2}e^{-\frac{\bar{C}(\kappa-S)}{S}}$, $0<S<\kappa$. The density function $P(x,t|x_0)\equiv P_s(x)\equiv e^{-x}$, $0<x<\infty$, is the Gamma density function $\mathrm{Gamma}(\nu,\theta)$ with $\nu=\theta=1$. The number $\bar{R}_0=1$ serves as a threshold at which the distribution $P(I,t|I_0)$ becomes stationary. The following graphs show how the distribution $P_s(I)$ changes with respect to the parameters κ and $\bar{C}$.

Fig. 1 (a) shows trajectories of $P_s(I)$ derived using different values $\bar{C}=0.3,1$, and 2, but fixed parameter $\kappa=1$, for the case $\bar{R}_0=1$. Fig. 1 (b) shows trajectories of $P_s(I)$ derived using different values $\kappa=0.3,0.5$, and 1, but fixed parameter $\bar{C}=1$, for the case $\bar{R}_0=1$. Here, we see that $\bar{C}$ is the shape parameter and κ is the location parameter.

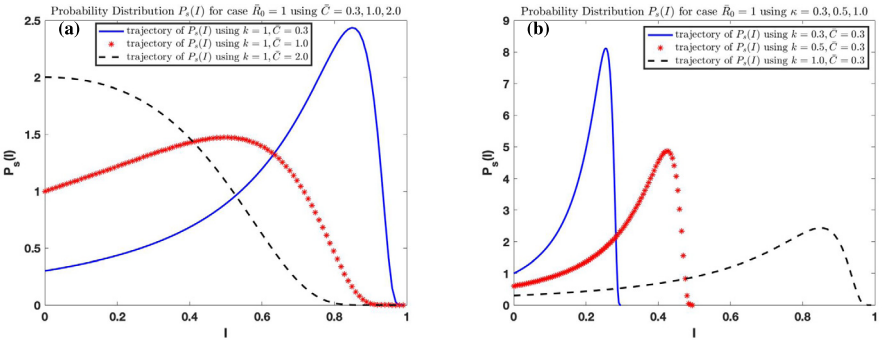

Fig. 1. Graphs of the probability distribution $P(I,t|I_0) = P_s(I)$ for the case where $\bar{R}_0 = 1$.

We can estimate statistically the parameters κ and $\bar{C}$ using sample of N independent identically distributed random variables $\{I_1, I_2, \cdots I_N\}$ of the stochastic process. Using the maximum likelihood estimation techniques, we find the maximum likelihood estimates $\hat{\bar{C}}$ and $\hat{\kappa}$ of $\bar{C}$ and κ satisfy

$$\begin{cases} \hat{\bar{C}} &= \left(\frac{1}{N}\sum_{j=1}^{N}\frac{I_j}{\hat{\kappa}-I_j}\right)^{-1}, \\ 0 &= \frac{N}{\hat{\kappa}} + \hat{\bar{C}}\sum_{j=1}^{N}\frac{I_j}{(\hat{\kappa}-I_j)^2} - 2\sum_{j=1}^{N}\frac{1}{\hat{\kappa}-I_j}. \end{cases}$$

Define

$$s_{\pm} = \frac{(2-\bar{\mathcal{A}}-\bar{C})\kappa \pm \sqrt{(2-\bar{\mathcal{A}}-\bar{C})^2\kappa^2 + 8\bar{\mathcal{A}}\kappa^2}}{4}. \tag{3.37}$$

In this case, the probability distribution $P_s(I)$ is increasing and decreasing on the intervals (s_-, s_+) and $(0,\kappa)\backslash(s_-,s_+)$, respectively.

From (3.20), it follows that the probability distribution exists if $\bar{R}_0 - 1 = \frac{\beta\kappa-(\mu+\gamma)-\sigma^2\kappa^2/2}{\mu+\gamma} \geq 0$ and do not exist if $\bar{R}_0 - 1 < 1$.

Remark 3. Effect of noise in the system. As the noise intensity in the transmission rate of disease increases (that is, as $\sigma \to \infty$), we see that $\bar{\mathcal{A}} \to -1$ (and hence $M \to 0$), $\bar{B} \to 1$, $\bar{C} \to 0$ and the probability distribution $P(I,t|I_0)$ behaves like the probability density function $P_{\sigma_\infty}(I) = \frac{\epsilon}{I(\kappa-I)}$, where $\epsilon = \lim_{\sigma\to\infty}\frac{\kappa\bar{C}^{\bar{\mathcal{A}}+1}}{\Gamma(\bar{\mathcal{A}}+1)}$. This effect is shown numerically in Fig. 4. This distribution is the special case of the Beta distribution, Beta(a,b), where $a = b = 0$. As $\sigma \to \infty$, the graph of the distribution concaves up with global minimum $4\epsilon/\kappa^2$ at $I = \kappa/2$ and increases (decreases) as $I > \kappa/2$ ($I < \kappa/2$). This distribution has no mean and variance. In summary, we conclude that increasing the noise intensity affects the distribution of the average number of infections in the system. The end-point behavior of the distribution suggests that as the noise intensity tends to ∞, the distribution $P(I,t|I_0) \to \infty$ as the number of infected individuals reduces to 0 or increases to total size of population, κ.

3.3.1. *Limiting distribution and statistics of the distribution* $P(I,t|I_0)$

It is easy to show that as $t \to \infty$,

$$\begin{aligned} P(I,t|I_0) &\to P_s(I), \\ \mu_I^{(1)}(t) &\to \frac{\kappa}{\Gamma(\bar{\mathcal{A}}+1)}\int_0^\infty \frac{u^{\bar{\mathcal{A}}+1}}{u+\bar{C}}e^{-u}\,du, \\ \sigma_I^2(t) &\to \frac{\kappa^2}{\Gamma(\bar{\mathcal{A}}+1)}\int_0^\infty \frac{u^{\bar{\mathcal{A}}+2}}{(u+\bar{C})^2}e^{-u}\,du - \frac{\kappa^2}{\Gamma(\bar{\mathcal{A}}+1)^2}\left(\int_0^\infty \frac{u^{\bar{\mathcal{A}}+1}}{u+\bar{C}}e^{-u}\,du\right)^2. \end{aligned} \tag{3.38}$$

The limiting skewness of the distribution can be calculated using the limit $\mu_I^{(j)}(t) \to \frac{\kappa^j}{\Gamma(\bar{\mathcal{A}}+1)}\int_0^\infty \frac{u^{\bar{\mathcal{A}}+j}}{(u+\bar{C})^j}e^{-u}\,du$ of the j-th moment. Also median$(t) \to \hat{m}$, where $\hat{m}$ is the solution of the equation

$$\frac{1}{\Gamma(\bar{\mathcal{A}}+1)}\int_0^{\frac{\bar{C}\hat{m}}{\kappa-\hat{m}}} u^{\bar{\mathcal{A}}-n}e^{-u}L(n,\alpha_n,u)\,du = 1/2.$$

The stationary distribution $P_s(I)$ is given in (3.36) and greatly studied in Mendez [10].

4. Results

We apply the distribution using the published influenza parameters in Mummert and Otunuga [11]. The parameters are associated with influenza data 'Influenza Positive Tests Reported to CDC by Public Health Laboratories' collected from the Center for Disease Control and Prevention (CDC[1]) Flu View for the thirteen influenza seasons 2004-2005 through 2016-2017.[2] The death rate, μ is collected from CIA.[3]

4.1. *Probability distribution of infection at time* t *for the case where* $\bar{R}_0 = 1$

In addition to the result in Fig. 1, we use published influenza parameters in Table 1 to show how the graph of the probability distribution $P(I,t|I_0 = 0.05)$ changes with respect to certain parameters. Fig. 2 **(a)**, **(b)**, **(c)** and **(d)** shows graphs of the probability distribution $P(I,t|I_0 = 0.05)$ derived using parameters ($\beta = 1.1252$, $\sigma = 0.5$; $M = 0$, $R_0 = 1.1250$), ($\beta = 1.5002$, $\sigma = 1$; $R_0 = 1.5$), ($\beta = 2.1252$, $\sigma = 1.5$; $R_0 = 2.1248$) and ($\beta = 4.1252$, $\sigma = 2.5$, $R_0 = 4.1244$), respectively. In each case, $\bar{R}_0 = 1$, $\kappa = 1$ and $M = \left\lfloor\frac{1}{2}(\bar{\mathcal{A}}+1)\right\rfloor = \lfloor 1/2\rfloor = 0$. From (3.19), the value $M = 0$ represents an eigenvalue of zero. In this case, the probability distribution $P(I,t|I_0 = 0.05)$ reduces to the one discussed in Remark 2. We note here that the distribution is not dependent on the transmission rate, β, since $\bar{\mathcal{A}} = 0$. We also note from Remark 2 that these graphs correspond to the stationary probability distribution $P_s(I)$ (with $\bar{\mathcal{A}} = 0$). The graph increases on the interval (s_-, s_+) and decreases on the interval $(0,\kappa)\backslash(s_-,s_+)$, where $s_\pm$ is defined in (3.37).

4.2. *Probability distribution of infection at time* t *for the case where* $M = 1$

Fig. 3 **(a)**, **(b)**, **(c)** and **(d)** shows the graphs of the probability distribution $P(I,t|I_0 = 0.05)$ of the number of infections at time t for the case $M = 1$ using parameters in Table 1 with ($\beta = 1.1127$; $\sigma = 0.3$; $M = 1$, $R_0 = 1.1125$), ($\beta = 1.5392$, $\sigma = 0.7$, $M = 1$, $R_0 = 1.5389$), ($\beta = 2.7747$, $\sigma = 1.3$, $M = 1$, $R_0 = 2.7741$), and ($\beta = 6.5547$, $\sigma = 2.3$, $M = 1$, $R_0 = 6.5534$), respectively.

4.3. *Probability distribution* $P(I,t|I_0)$ *showing the effect of noise in the system*

Fig. 4 **(a)**, **(b)**, **(c)** and **(d)** shows graphs of the probability distribution $P(I,t|I_0 = 0.05)$ of the number of infections at time t using parameters in Table 1 with ($\sigma = 1$; $\beta = 2$), ($\sigma = 2$; $\beta = 2$), ($\sigma = 4$; $\beta = 2$),

[1] http://www.cdc.gov/flu/professional/acip/clinical.htm.
[2] http://gis.cdc.gov/grasp/fluview/fluportaldashborad.html.
[3] CIA World Factbook, https://www.cia.gov/library/publications/the-world-factbook/.

Table 1
Parameter values selected from [11].

Parameter	Description	Value	Source
γ	temporary recovery rate (week^{-1})	1	[11]
μ	death rate (week^{-1})	0.0002	CIA[3]
Λ	recruitment rate (week^{-1})	μ	[11]
β	transmission rate	$[1.1, 455.6]$	(extracted from [11])
σ	noise intensity	$[0.04, 0.4] \times \beta$	(extracted from [11])

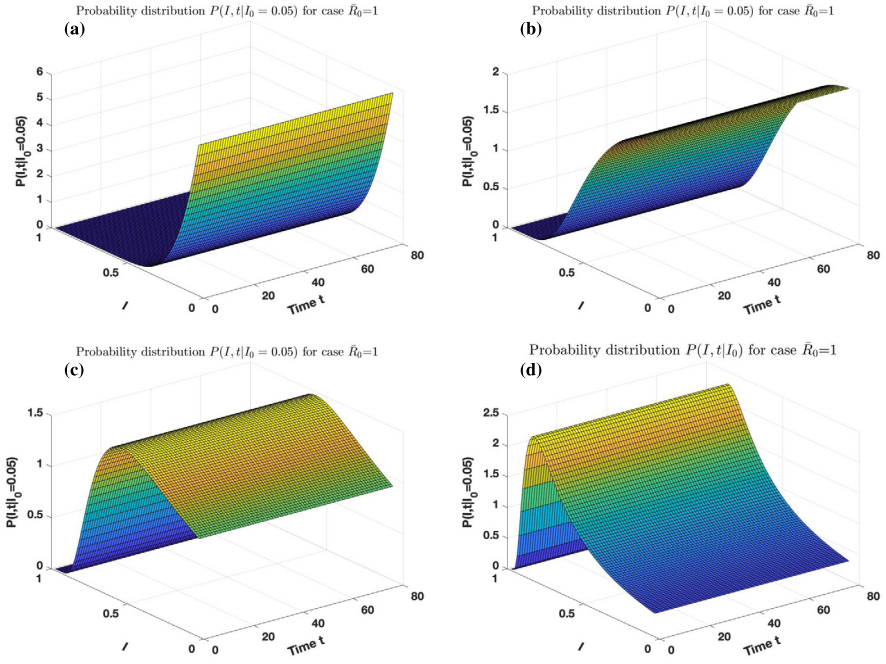

Fig. 2. Graphs of the probability distribution of Infection at time t for the case where $\bar{R}_0 = 1$.

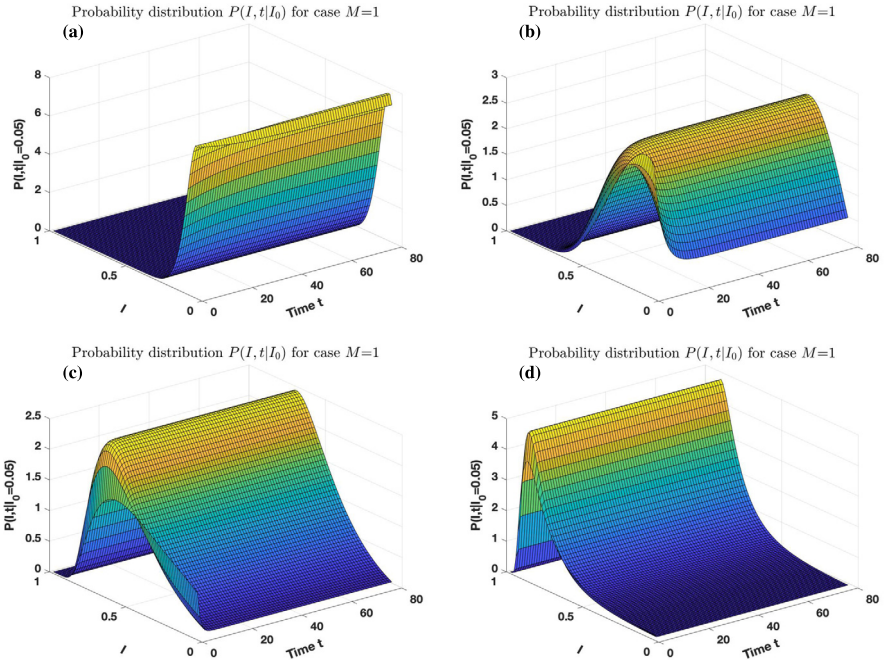

Fig. 3. Graphs of the probability distribution of Infection at time t for the case $M = 1$.

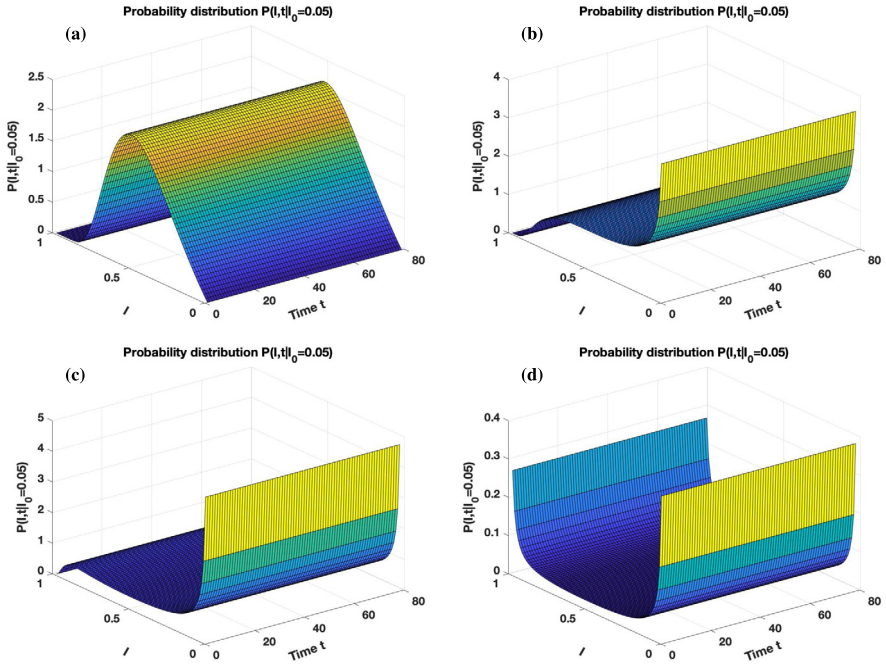

Fig. 4. Graphs of the probability distribution of Infection at time t showing the effect of noise in the system.

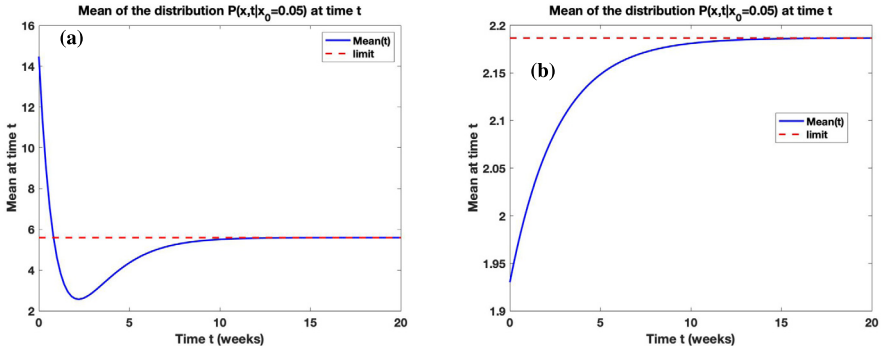

Fig. 5. Mean of the distribution $P(x,t|x_0)$ at time t.

and ($\sigma = 20$; $\beta = 2$), respectively. The Figure shows how the shape of the distribution changes as the noise intensity, σ, increases. We recall from Remark 3 that as $\sigma \to \infty$, $M \to 0$ and $P(I,t|I_0) \to \frac{\epsilon}{I(\kappa - I)}$. Here, σ behaves like the shape parameter.

4.4. Statistic results for the distribution $P(x,t|x_0)$)

Fig. 5 **(a)** and **(b)** shows the graphs of the mean of the distribution $P(x,t|x_0)$ at time t using parameters in Table 1 with ($\beta = 1.7$; $\sigma = 0.5$) and ($\beta = 1.7$; $\sigma = 0.8$), respectively. The thick line is the trajectory of the mean function, $\mu_x^{(1)}(t)$, given in (3.28) as a function of time, while the dashed line is the horizontal line representing the limit $\lim_{t\to\infty} \mu_x^{(1)}(t)$ of the mean function. This value is derived in (3.32) to be $\bar{\mathcal{A}} + 1$.

Fig. 6 **(a)** and **(b)** shows the graphs of the variance of the distribution $P(x,t|x_0)$ at time t using parameters in Table 1 with ($\beta = 1.7$; $\sigma = 0.5$) and ($\beta = 1.7$; $\sigma = 0.8$), respectively. The thick line is the trajectory of the variance function, $\sigma_x^2(t)$, given in (3.28) as a function of time, while the dashed line is the horizontal line representing the limit $\lim_{t\to\infty} \sigma_x^2(t)$ of the variance function. This value is derived in (3.32) to be $\bar{\mathcal{A}} + 1$.

Fig. 7 **(a)** and **(b)** shows the graphs of the skewness of the distribution $P(x,t|x_0)$ at time t using parameters in Table 1 with ($\beta = 1.7$; $\sigma = 0.5$) and ($\beta = 1.7$; $\sigma = 0.8$), respectively. The thick line is the trajectory of the skewness function, $\mathrm{sk}_x(t)$, given in (3.28) as a function of time, while the dashed line is the horizontal line representing the limit $\lim_{t\to\infty} \mathrm{sk}_x(t)$ of the skewness function. This value is derived in (3.32) to be $2\left(\bar{\mathcal{A}} + 1\right)^{-1/2}$.

Fig. 8 **(a)** and **(b)** shows the graphs of the mode of the distribution $P(x,t|x_0)$ at time t using parameters in Table 1 with ($\beta = 2$; $\sigma = 0.4$), ($\beta = 2.7$; $\sigma = 0.6$), respectively. The thick line is the trajectory of the mode function, $\mathrm{mode}_x(t)$, described in (3.29), while the dashed line is the horizontal line representing the limit $\lim_{t\to\infty} \mathrm{mode}_x(t)$ of the mode function given in (3.32) to be $\bar{\mathcal{A}}$.

Fig. 9 **(a)** and **(b)** shows the graphs of the median of the distribution $P(x,t|x_0)$ at time t using parameters in Table 1 with ($\beta = 1.7$; $\sigma = 0.5$), ($\beta = 2$; $\sigma = 0.5$), respectively. The thick line is the trajectory of the median function, $\mathrm{median}_x(t)$, described in (3.30), while the dashed line is the horizontal line representing the limit $\lim_{t\to\infty} \mathrm{median}_x(t)$ of the median function.

4.5. Statistic results for the distribution $P(I,t|I_0 = 0.05)$)

Fig. 10 **(a)** and **(b)** shows the graphs of the mean of the distribution $P(I,t|I_0)$ at time t using parameters in Table 1 with ($\beta = 1.7$; $\sigma = 0.5$) and ($\beta = 1.7$; $\sigma = 0.8$), respectively. The thick line is the trajectory of the mean function, $\mu_I^{(1)}(t)$, described in (3.34), while the dashed line is the

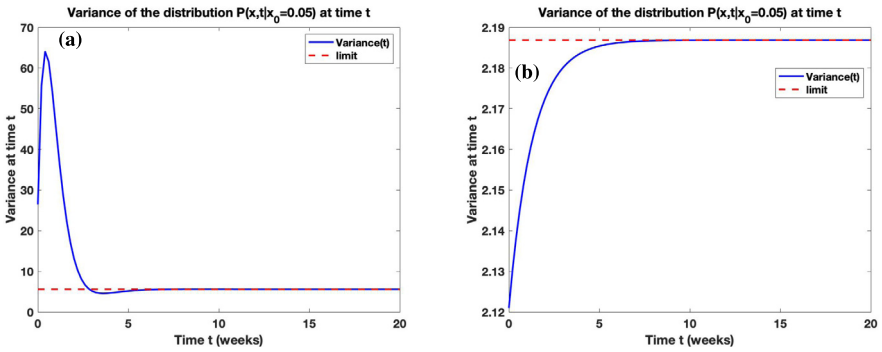

Fig. 6. Variance of the distribution $P(x,t|x_0)$ at time t.

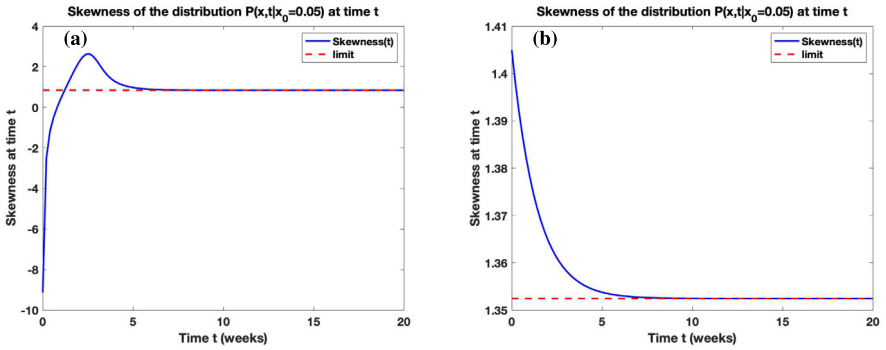

Fig. 7. Skewness of the distribution $P(x,t|x_0)$ at time t.

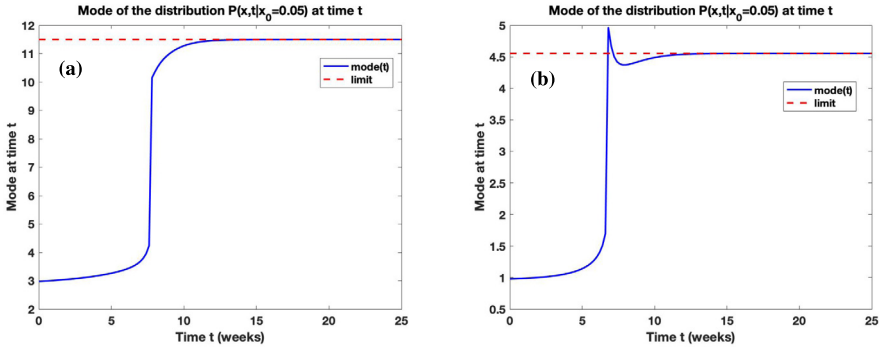

Fig. 8. Mode of the distribution $P(x,t|x_0)$ at time t.

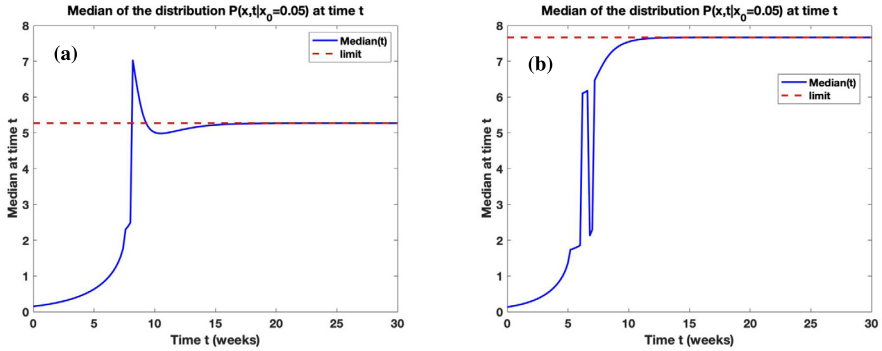

Fig. 9. Median of the distribution $P(x,t|x_0)$ at time t.

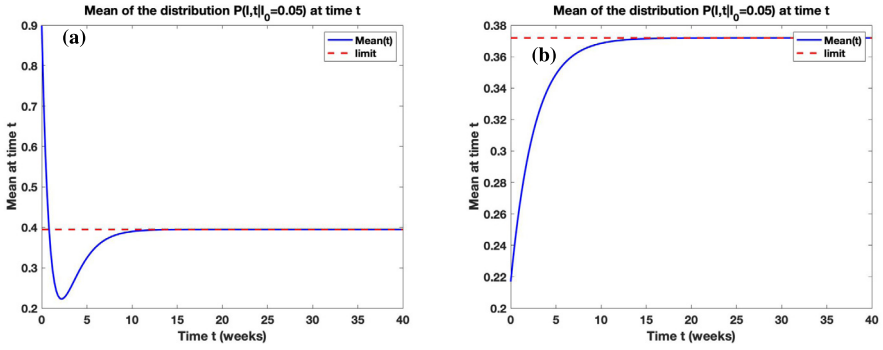

Fig. 10. Mean of the distribution $P(I,t|I_0)$ at time t.

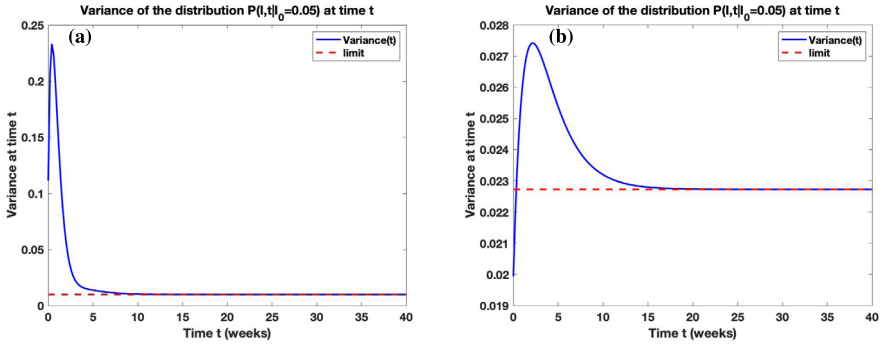

Fig. 11. Variance of the distribution $P(I,t|I_0)$ at time t.

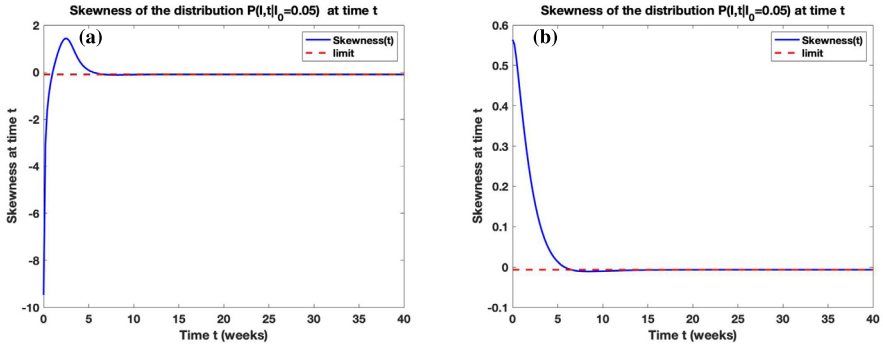

Fig. 12. Skewness of the distribution $P(I,t|I_0)$ at time t.

horizontal line representing the limit $\lim_{t\to\infty}\mu_I^{(1)}(t)$ of the mean function described in (3.38).

Fig. 11 **(a)** and **(b)** shows the graphs of the variance of the distribution $P(I,t|I_0)$ at time t using parameters in Table 1 with ($\beta = 1.7$; $\sigma = 0.5$) and ($\beta = 1.7$; $\sigma = 0.8$), respectively. The thick line is the trajectory of the variance function, $\sigma_I^2(t)$, given in (3.34) as a function of time, while the dashed line is the horizontal line representing the limit $\lim_{t\to\infty}\sigma_I^2(t)$ of the variance function. This value is derived in (3.38).

Fig. 12 **(a)** and **(b)** shows the graphs of the skewness of the distribution $P(I,t|I_0)$ at time t using parameters in Table 1 with ($\beta = 1.7$; $\sigma = 0.5$) and ($\beta = 1.7$; $\sigma = 0.8$), respectively. The thick line is the trajectory of the skewness function, $\text{sk}_I(t)$, given in (3.34) as a function of time, while the dashed line is the horizontal line representing the limit $\lim_{t\to\infty}\text{sk}_I(t)$ of the skewness function described in Section 3.3.1.

Fig. 13 **(a)** and **(b)** shows the graphs of the mode of the distribution $P(I,t|I_0)$ at time t using parameters in Table 1 with ($\beta = 2$; $\sigma = 0.5$), ($\beta = 2.7$; $\sigma = 0.7$), respectively. The thick line is the trajectory of the mode function, $\text{mode}_I(t)$, described in Subsection 3.3, while the dashed line is the horizontal line representing the limit $\lim_{t\to\infty}\text{mode}_I(t)$ of the mode function given in Section 3.3.1.

Fig. 14 **(a)** and **(b)** shows the graphs of the median of the distribution $P(I,t|I_0)$ at time t using parameters in Table 1 with ($\beta = 1.7$; $\sigma = 0.5$), ($\beta = 2$; $\sigma = 0.5$), respectively. The thick line is the trajectory of the mode function, $\text{median}_I(t)$, described in Subsection 3.3, while the dashed line is the horizontal line representing the limit $\lim_{t\to\infty}\text{median}_I(t)$ of the mode function given in Section 3.3.1.

5. Conclusion

We studied how infection is being distributed in a population. By extending the well known deterministic SIS model into a stochastic model, we derive the closed form probability distribution of the number of infected individuals at a particular time t using the Fokker-Planck equation. Under certain transformation, the differential equation governing the probability density function (PDF) reduces to a Kummer/Laguerre differential equation. As the noise intensity σ increases, the distribution $P(I,t|I_0)$ behaves like the Beta distribution Beta(0,0). Increasing

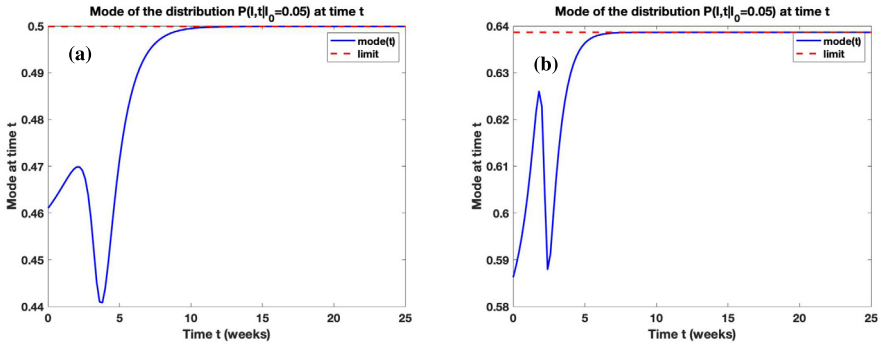

Fig. 13. Mode of the distribution $P(I,t|I_0)$ at time t.

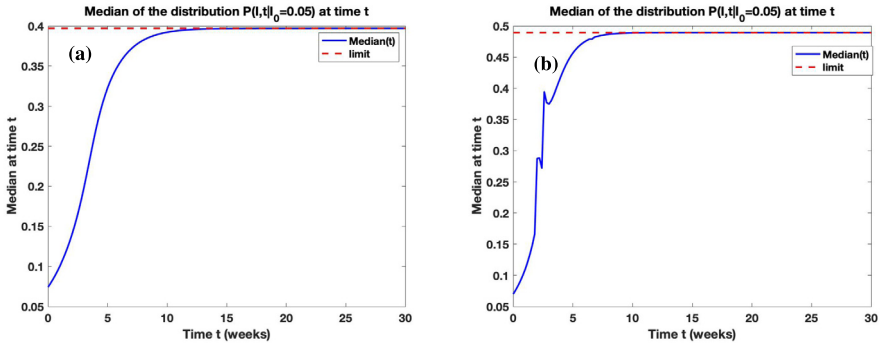

Fig. 14. Median of the distribution $P(I,t|I_0)$ at time t.

the noise intensity σ affects the distribution of the number of infections. We note that the stationary probability distribution $P_s(I)$ exists only for the case where $R_0 > 1$, where R_0 is defined in (1.4) as the average number of secondary infection produced by an infected individual when introduced into a completely susceptible population. Also, we showed that the number $\bar{R}_0 = 1$ serves as a threshold at which the distribution $P(I,t|I_0)$ becomes stationary distribution $P_s(I)$, and that the distribution increases (decreases) in this case on the interval (s_-, s_+) $((0,\kappa)\backslash(s_-,s_+))$. The limiting distribution and statistics of the distribution at time t are calculated. The result is applied to U.S. Influenza data for the seasons 2004-2017.

Declarations

Author contribution statement

Olusegun Michael Otunuga: Conceived and designed the analysis; Analyzed and interpreted the data; Contributed analysis tools or data; Wrote the paper.

Funding statement

This research did not receive any specific grant from funding agencies in the public, commercial, or not-for-profit sectors.

Competing interest statement

The authors declare no conflict of interest.

Additional information

No additional information is available for this paper.

References

[1] M. Abramowitz, I.A. Stegun, Handbook of Mathematical Functions with Formulas, Graphs, and Mathematical Tables, Dover Publications, Inc., NY, U.S.A., 1965.
[2] L. Arnold, Stochastic Differential Equations: Theory and Applications, Wiley, New York, 1974.
[3] Christine Bernadi, Yvon Madday, James F. Blowey, John P. Coleman, Alan W. Craig, Theory and Numerics of Differential Equations, Springer-Verlag, Berlin Heidelberg, 2001.
[4] A. Gray, D. Greenhalgh, L. Hu, X. Mao, J. Pan, A stochastic differential equation SIS epidemic model, SIAM J. Appl. Math. 71 (3) (2011) 876–902.
[5] A. Erdelyi, Higher Transcendental Functions, vols. 1 and 2, McGraw-Hill, New York, 1953.
[6] W. Horsthemke, R. Lefever, Noise-Induced Transitions. Theory and Applications in Physics, Chemistry, and Biology, Springer-Verlag, Berlin Heidelberg, 1984.
[7] S. Iyanaga, Y. Kawada, Encyclopedia Dictionary of Mathematics, MIT Press, Cambridge, MA, 1980.
[8] P.E. Kloeden, E. Platen, Numerical Solution of Stochastic Differential Equations, Springer-Verlag, New York, 1995.
[9] Q. Liu, D. Jiang, N. Shi, T. Hayat, Dynamics of a stochastic delayed SIR epidemic model with vaccination and double diseases driven by Levy jumps, Physica A 492 (2018) 2010–2018.
[10] V. Méndez, D. Campos, W. Horsthemke, Stochastic fluctuations of the transmission rate in the susceptible-infected-susceptible epidemic model, Phys. Rev. E 86 (2012) 011919.
[11] Anna Mummert, O.M. Otunuga, Parameter identification for a stochastic SEIRS epidemic model: case study influenza, J. Math. Biol. 79 (2) (2019) 705–729.
[12] F.W. Olver, D.W. Lozier, R.F. Boisvert, C.W. Clark, NIST Handbook of Mathematical Functions, National Institute of Sciences and Technology, U.S. Department of Commerce and Cambridge University Press, Dubai, Tokyo and New York U.S.A., 2010.
[13] O.M. Otunuga, Global stability for a $2n+1$ dimensional HIV/AIDS epidemic model with treatments, Math. Biosci. 299 (2018) 138–152.
[14] O.M. Otunuga, Global stability of nonlinear stochastic SEI epidemic model, Int. J. Stoch. Anal. 2017 (2017), 6313620, pp. 1–7.
[15] Elisabetta Tornatore, Stefania Maria Buccellato, Pasquale Vetro, Stability of a stochastic SIR system, Physica A 354 (2005) 111–126.
[16] B.J. West, A.R. Bulsara, K. Lindenberg, V. Seshadri, K.E. Shuler, Stochastic processes with non-additive fluctuations: I. Itô and Stratonovich calculus and the effects of correlations, Physica A 97 (2) (1979) 211–233.

[17] E.T. Whittaker, G.N. Watson, A Course in Modern Analysis, 4th ed., Cambridge University Press, Cambridge, England, 1990.
[18] P.J. Witbooi, Stability of an SEIR epidemic model with independent stochastic perturbations, Physica A 392 (2013) 4928–4936.
[19] E. Wong, The construction of a class of stationary Markoff processes, Proc. Symp. Appl. Math. 16 (1964) 264.
[20] E. Wong, M. Zakai, On the convergence of ordinary integrals to stochastic integrals, Ann. Math. Stat. 36 (5) (1965) 1560–1564.
[21] Xiao-Bing Zhang, S. Chang, Q. Shi, Hai-Feng Huo, Qualitative study of a stochastic SIS epidemic model with vertical transmission, Physica A 505 (2018) 805–817.
[22] X. Zhang, K. Wang, Stochastic SEIR model with jumps, Appl. Math. Comput. 239 (2014) 133–143.
[23] Yanli Zhou, Weiguo Zhang, Threshold of a stochastic SIR epidemic model with Levy jumps, Physica A 446 (2018) 204–216.
[24] X. Zhong, F. Deng, Dynamics of a stochastic multigroup SEIR epidemic model, J. Appl. Math. (2014) 258915, 5pp.